

Fast Quantum State Tomography in the Nitrogen Vacancy Center of Diamond

Jingfu Zhang¹, Swathi S. Hegde,^{*} and Dieter Suter¹

Fakultät Physik, Technische Universität Dortmund, D-44221 Dortmund, Germany

 (Received 30 August 2021; revised 11 November 2022; accepted 20 January 2023; published 28 February 2023)

Quantum state tomography is the procedure for reconstructing unknown quantum states from a series of measurements of different observables. Depending on the physical system, different sets of observables have been used for this procedure. In the case of spin qubits, the most common procedure is to measure the transverse magnetization of the system as a function of time. Here, we present a different scheme that relies on time-independent observables and therefore does not require measurements at different evolution times, thereby greatly reducing the overall measurement time. To recover the full density matrix, we use a set of unitary operations that transform the density operator elements into the directly measurable observable. We demonstrate the performance of this scheme in the electron-nuclear spin system of the nitrogen vacancy center in diamond.

DOI: [10.1103/PhysRevLett.130.090801](https://doi.org/10.1103/PhysRevLett.130.090801)

Introduction.—Finding the state of a quantum system is one of the main tasks for many applications in basic quantum physics [1] as well as in many emerging quantum technologies, such as in the field of quantum information [2,3]. Using quantum state tomography (QST), one can reconstruct the quantum state represented by a density operator, which contains the full information about the system [2,4,5]. Performing a full QST requires serial measurements of a complete set of observables. The size of such a complete set and therefore the number of individual measurements and the measurement time all grow exponentially with the number of qubits in the system.

While QST has been performed for many years [6,7], it was often done in the form of time-dependent measurements [8,9]. In spin-based systems such as nuclear magnetic resonance [3,10], it is often not possible or not optimal to use projective measurements. Instead, the established procedure relies on the measurement of free induction decays (FIDs) [6,7], which may generate information on multiple density operator elements in a single scan [8,11,12]. This procedure has therefore been well established in ensemble quantum information processing.

In the case of single spin qubits such as the nitrogen vacancy (NV) center in diamond [13,14], this type of measurement is also applicable [9,15], but the precessing transverse magnetization that is detected in a conventional FID experiment is not directly observable. Instead, the transverse magnetization (coherence) has to be converted into population of the electron spin and detected as a change of the photoluminescence count rate; this is known as the Ramsey-fringe method [14]. Since this type of readout results in a large number of individual measurements, the procedure becomes even more time-consuming. Therefore, we propose here a different approach that is significantly more efficient for this type of qubit:

eliminating the need for free evolution reduces the number of actual measurements by several orders of magnitude, with a corresponding reduction of the overall measurement time.

In our scheme, the photon count rate is the immediate observable; it is directly connected to populations of the electron spin, which correspond to the diagonal elements or their linear combination in the density matrix. Since such populations do not change during free evolution, the observable is not time-dependent. The other elements of the density matrix can be transformed to the observable through unitary transformations. With a suitable decomposition of the density operator, every element in the basis set can be converted into the observable and therefore be read out by a single measurement. Overall, this procedure provides a dramatic speedup by several orders of magnitudes, compared to the measurement of precessing magnetization. As an experimental demonstration, we implement this procedure in the single NV center of diamond, which is used in many emerging applications of quantum information and sensing technologies. [14,16–20].

Single-qubit state tomography.—We start with the QST of single qubit [21–24]. We consider systems where the measurement of diagonal density operator elements is easy, such as in the NV centers of diamond where the populations can be determined by photon counting [14]. In the case of single qubits, the relevant Hilbert space is spanned by the computational basis $\{|0\rangle, |1\rangle\}$, which are the eigenstates of the Pauli operator Z with eigenvalues ± 1 . The density matrix describing the quantum state can be expanded in terms of the unit operator E and the Pauli matrices (X , Y , and Z) as

$$\rho = c_E E + c_X X + c_Y Y + c_Z Z, \quad (1)$$

where $c_E = 1/2$ for a normalized density operator and the other c_i are the weights of the corresponding Pauli matrices. The diagonal elements ρ_{11} and ρ_{22} , which correspond to the populations $p_{|0\rangle}$ and $p_{|1\rangle}$ of the states $|0\rangle$ and $|1\rangle$, are related to the coefficients c_E and c_Z as

$$c_E = 1/2 = (p_{|0\rangle} + p_{|1\rangle})/2, \quad c_Z = (p_{|0\rangle} - p_{|1\rangle})/2. \quad (2)$$

To measure the off-diagonal elements of the density operator ρ , we apply operations X_{90} and Y_{90} to transform them to diagonal elements. Here, X_α and Y_α are rotations of the qubit around the x - and y - axis by an angle α . They transform $c_Y Y$ and $c_X X$ to $c_Y Z$ and $-c_X Z$, respectively. Therefore, c_X and c_Y can be measured directly in the transformed states.

For the experimental demonstration, we used the electron spin of a single NV center in a diamond sample with natural abundance ($\sim 1.1\%$) of ^{13}C . The experiments were performed at room temperature. The static magnetic field B was aligned along the symmetry axis of the NV center. The relevant Hamiltonian of the electron spin is then $\mathcal{H}_e/(2\pi) = DS_z^2 - B\gamma_e S_z$. Here, S_z denotes the spin-1 operator for the electron, D the zero-field splitting, and γ_e the gyromagnetic ratio [14]. Figure 1 shows the pulse sequence, which always starts with the polarization of the electron spin into the state $m_S = 0$, using a pulse of a 532 nm laser. The polarization is higher than 70% [21], and in the present work we can approximate the pseudopure state as a pure state $|0\rangle$ as discussed in the Supplemental Material (SM, Sect. IC) [25].

The population of the state $m_S = 0$ can be measured by the count rate r of the fluorescence detected during a second laser pulse, since the state $m_S = 0$ fluoresces more strongly than $m_S = \pm 1$ [14,21,34,35]:

$$r = r_{\min} + p_{|0\rangle}(r_{\max} - r_{\min}). \quad (3)$$

The maximum count rate r_{\max} corresponds to the system being in state $m_S = 0$, while the minimum count rate r_{\min} results when the system is in $m_S = \pm 1$. The readout is destructive, since the laser pumps the system back to the state $|0\rangle$. Therefore, the measurement time has to be kept relatively short [14] to obtain a good measure of the

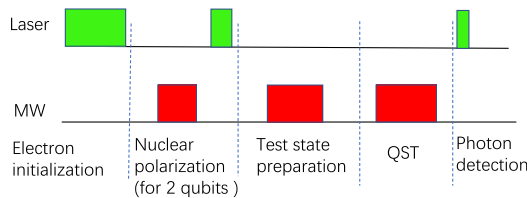


FIG. 1. Pulse sequence for state preparation followed by QST. The nuclear spin polarization step is only used for the 2-qubit system. Each green box represents a laser pulse, while the red boxes represent sequences microwave (MW) pulses.

instantaneous population. To reduce the effects of drift and laser power fluctuations, we always calibrate the count rate against a measurement of r_{\max} obtained after repumping the system to the $m_S = 0$ state.

The single qubit is obtained from the electron spin states $m_S = 0$ and $m_S = -1$, which we identify with the two logic states $|0\rangle$ and $|1\rangle$. For the 1-qubit case, the test state preparation and the transformations for the QST were implemented by single microwave (MW) pulses with a Rabi frequency of 9 MHz. The measured count rate r then allows us to determine the populations of the state as

$$p_{|0\rangle} = (r - r_{\min})/\delta_r, \quad p_{|1\rangle} = (r_{\max} - r)/\delta_r, \quad (4)$$

where $\delta_r \equiv r_{\max} - r_{\min}$. Writing r_N , r_X , and r_Y for the count rates measured after the 3 operations NOOP (no operation), X_{90} and Y_{90} we obtain the coefficients

$$\begin{aligned} c_X &= (1/2) - (r_Y - r_{\min})/\delta_r \\ c_Y &= (r_X - r_{\min})/\delta_r - (1/2) \\ c_Z &= (r_N - r_{\min})/\delta_r - (1/2). \end{aligned} \quad (5)$$

To test the QST procedure, we first prepared test states $|0\rangle$, $|1\rangle$, $|+\rangle = (|0\rangle + |1\rangle)/\sqrt{2}$, and $|-\rangle = (|0\rangle - i|1\rangle)/\sqrt{2}$ by applying the operations NOOP, X_{180} , Y_{90} , and X_{90} to state $|0\rangle$, respectively. These states are eigenstates of the Pauli matrices Z , X , and Y .

Figure 2 shows a graphical representation of the density matrices, reconstructed from the measured coefficients, whose values are given in the SM [25]. The top row shows the real parts of the density matrices for states $|0\rangle$, $|1\rangle$, and $|+\rangle$. The bottom row shows the real and imaginary parts for state $|-\rangle$.

From the reconstructed density operators, we calculated the fidelity [36]

$$F = \frac{\text{Tr}\{\rho^{\text{th}}\rho^{\text{exp}}\}}{\sqrt{\text{Tr}\{\rho^{\text{th}}\rho^{\text{th}}\}\text{Tr}\{\rho^{\text{exp}}\rho^{\text{exp}}\}}}, \quad (6)$$

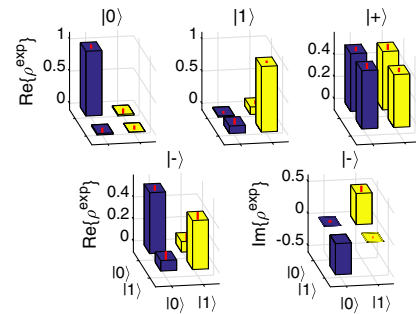


FIG. 2. Experimental results of the tomography of a single qubit. The top row shows the real parts of the measured density matrices for states $|0\rangle$, $|1\rangle$, and $|+\rangle$, as indicated in the panel. The bottom row shows the real and imaginary parts for state $|-\rangle$. The error bars show the standard deviations obtained by repeating the measurements.

where ρ^{th} and ρ^{exp} are the theoretical and experimentally reconstructed density operators. The resulting fidelities for the input states $|0\rangle$, $|1\rangle$, $|+\rangle$, and $|-\rangle$ are 0.994, 0.985, 0.995, and 0.986, respectively. The deviation between experiment and theory can be mainly attributed to the statistics of the photon detection and the control errors (pulse imperfection) in implementing the state preparation and tomography. Compared with the fidelity for state $|0\rangle$, the slightly lower fidelities for the other three states can be used to estimate the process fidelity of the state preparation.

For a second example of 1-qubit QST, we identified the qubit again with the same electronic spin states $m_S = 0$ and $m_S = -1$, but now conditional on the ^{14}N nuclear spin being in the $m_N = 1$ state. The experiments were performed in a center in the ^{12}C enriched (99.995%) diamond sample [37–39]. We obtained a slightly higher fidelity than the earlier experiments. The results are presented in the SM [25].

State tomography for 2 qubits.—Moving to a 2-qubit system, we use the basis states $\{|00\rangle, |01\rangle, |10\rangle, |11\rangle\}$ and we expand the density operator in a basis of products of single qubit operators:

$$\rho = \sum_{m,n=1}^4 c_{mn} a_m \otimes b_n, \quad (7)$$

where $a_m, b_n \in \{E, X, Y, Z\}$ represent the unit operator E and the Pauli matrices acting on one of the qubits. Since the trace of a normalized density operator is unity, the coefficient $c_{EE} = 1/4$ is fixed. The goal of the tomography is to determine the other 15 coefficients c_{mn} .

The primary observable for measuring populations is again the photon count rate, which depends on the state of the electron spin before the readout pulse is applied, but is independent of the state of the nuclear spin. The measured count rate is then, in analogy to Eq. (3),

$$r = r_{\min} + (p_{|00\rangle} + p_{|01\rangle})(r_{\max} - r_{\min}). \quad (8)$$

Equation (4) also holds, with $p_{|0\rangle} \rightarrow p_{|00\rangle} + p_{|01\rangle}$ and $p_{|1\rangle} = p_{|10\rangle} + p_{|11\rangle}$. Therefore,

$$p_{|00\rangle} + p_{|01\rangle} = (r_N - r_{\min})/\delta_r \quad (9)$$

$$p_{|10\rangle} + p_{|11\rangle} = (r_{\max} - r_N)/\delta_r \quad (10)$$

and

$$c_{ZE} = (r_N - r_{\min})/(2\delta_r) - (1/4), \quad (11)$$

which corresponds to c_Z in Eq. (5) in the single qubit QST.

To determine the remaining coefficients of the density operator, we apply a set of unitary operations R to transform the relevant operators $c_{mn} a_m b_n$ to $c_{mn} ZE$. The coefficient c_{mn} in the transformed density matrix can be

directly measured using Eq. (11), by replacing r_N by r_R , where $r_R = 2\delta_r[c_{mn} + (1/4)] + r_{\min}$ denotes the count rate measured from the transformed density matrix. Overall we can use 15 measurements to obtain the 15 coefficients, i.e., one measurement for each element of the density operator.

To demonstrate the 2-qubit scheme, we used the electron spin coupled to a single ^{13}C nuclear spin, where the electron spin in states $m_S = 0$ and $m_S = -1$ was assigned as qubit 1 and ^{13}C nuclear spin qubit 2. We used a ^{12}C enriched (99.995%) diamond to minimize decoherence due to additional ^{13}C nuclear spins [39]. In this context, we focus on the electron and ^{13}C subsystem with the ^{14}N in the state $m_N = +1$. The pulse sequence is shown in Fig. 1, with more details given in the SM [25]. The required operations can be efficiently generated by applying a small number of MW pulses acting on the electron spin, combined with free precession [40–45].

To prepare the pure state $|00\rangle$, we first polarized the electron spin, swapped the states of the two qubits and repolarized the electron spin [42,43]. Additional details are provided in the SM [25]. We implemented $X_{90} \otimes E$, $Y_{90} \otimes E$, and $X_{180} \otimes E$ by single MW pulses. The other required unitaries were implemented by pulse sequences that were designed by optimal control theory [42,46]. These pulse sequences transfer the target operators to ZE with fidelities of ≥ 0.99 . The pulse sequences consist of up to 3 MW pulses and the same number of free precession periods and total durations up to 15 μs , which is short compared to the transverse relaxation times $T_2 = 700 \mu\text{s}$ and $T_2^* = 40 \mu\text{s}$ of the electron spin. Additional details are given in the SM [25].

As experimental demonstrations, we reconstruct the density matrices of the following states: $s_1 = |00\rangle$, $s_2 = |0\rangle(|0\rangle + |1\rangle)/\sqrt{2}$, $s_3 = (|00\rangle + |11\rangle)/\sqrt{2}$, and $s_4 = (|01\rangle + |10\rangle)/\sqrt{2}$. The states s_2 – s_4 were generated by applying sequences of MW pulses and delays to $|00\rangle$. Each sequence consists of three pulses and three delays. The theoretical fidelity of the generated state is > 0.99 .

The experimental results for the real parts of the measured density matrices are illustrated in Fig. 3. The rms values of imaginary parts in the experimental density operator are 0.028, 0.033, 0.039, and 0.026, for the input states s_1 – s_4 , respectively. We present the measured imaginary parts of the density matrices in the SM [25].

The experimental fidelities for the states s_1 – s_4 , are 0.98, 0.97, 0.97, and 0.97, respectively. The main contributions to the deviation from unity are (i) dephasing (0.05%), (ii) the theoretical imperfections of the pulse sequences (1%), (iii) experimental imperfections of the MW pulses (1%), and (iv) photon counting statistics (2%). Additional details are presented in the SM (Sect. VC) [25]. We are currently optimizing the conversion sequences such that they combine high fidelity for the unitary conversion operation with suppression of dephasing [40,47].

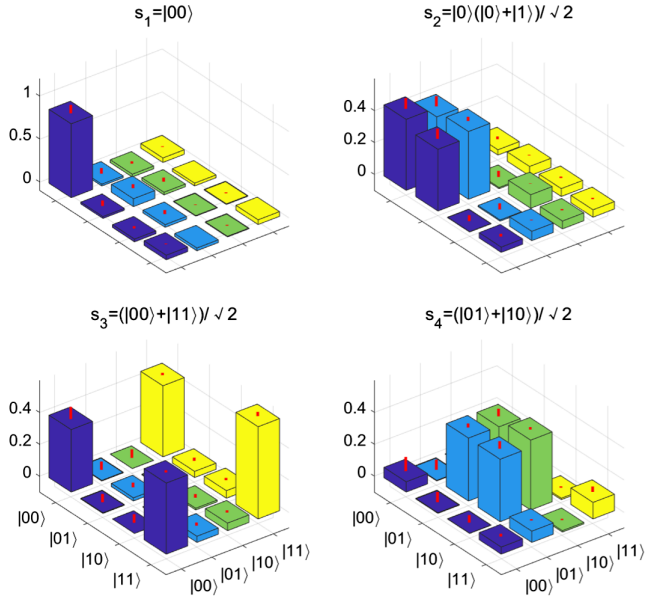


FIG. 3. Real parts of the density matrices experimentally reconstructed by the QST for the input states s_1 – s_4 .

Discussion.—Our scheme can be straightforwardly generalized to the multiple qubit system. In a n qubit system, the observable is $\underbrace{ZE\dots E}_{n-1}$, denoting a product operator with Z for the electron spin qubit and E for the $n-1$ nuclear spin qubits. Equation (11) is generalized to

$$c_{\underbrace{ZE\dots E}_{n-1}} = (r_N - r_{\min}) / (2^{n-1} \delta_r) - (1/2^n). \quad (12)$$

In a similar way, all product operators can be transformed to $\underbrace{ZE\dots E}_{n-1}$ by unitary operations. Therefore, we need $(2^{2n} - 1)$ measurements for reconstructing the full density operator. More details are presented in the SM (Sect. VE) [25]. The number of measurements required by the time-dependent experiments (Ramsey) also increases proportionally to the number of elements in the density operator. While the precise number depends on the details of the coupling network, additional couplings allow one to extract more density matrix elements from a single FID measurement and therefore reduce the number of FIDs that must be measured [8]. On the other hand, they lead to increased spectral crowding, which requires a larger number of points per FID. As a result, the time saving of the time-independent over the time-dependent approach does not depend on the number of qubits. More details are shown in the SM (Sect. VE) [25]. We therefore conclude that the time saving of > 2 orders of magnitude should be similar for all relevant quantum registers. However, full QST for systems with > 3 qubits will probably remain impractical even with this faster method.

Conclusion.—Quantum state tomography is an essential tool for the analysis of quantum mechanical systems as it allows one to extract all available information [1–3]. Accordingly, efficient procedures for QST are valuable for a vast range of applications where information on multiple density operator elements is accessed [48]. Early QST experiments, e.g., in quantum optics [4,5], were based on measurements in different bases to extract the coefficients of the density operator components. In the system that we are considering, only a single observable is available. To access different density operator components, we therefore convert them into the available observable through a set of unitary transformations. Early QST experiments by liquid-state NMR [12] also used a single measurement basis, but since the relevant measurement is not projective, it was possible to continuously monitor the time evolution of the density operator, which converts density operator components that are not directly observable into the observable one [6,49]. In the case of QST of single spins in solids, the evolution of coherences cannot be observed directly; it was therefore replaced by indirect detection using the Ramsey method [49]. While this approach allowed one to transfer the techniques developed for liquid-state NMR to the single-spin systems, it generates a huge overhead, since a single measurement is replaced by a sequence of typically several hundred measurements with different evolution times. In the method presented here, we remove this overhead, which allows a speedup of the QST by several orders of magnitude compared to the measurement of time-dependent observables for both the number of required measurements and the overall measurement time (see SM, Sect. VD) [25]. Similar to the existing procedures, the reconstruction of the density operator can be improved by combing the measurement results with statistical inference methods that result in a density matrix that is close to the physical state [50–55]. Since QST is the main prerequisite for quantum process tomography [56,57], our method is also very helpful for speeding up this tomography. For our experimental demonstration, we used a nitrogen vacancy center in diamond, but the scheme should be equally applicable to other physical systems, such as photons, atomic ensembles, and trapped ions [5,58–60].

This project has received funding from the European Union’s Horizon 2020 research and innovation programme under Grant agreement no. 828946. The publication reflects the opinion of the authors; the agency and the commission may not be held responsible for the information contained in it. We thank Sven Lauhof for the help in the experiment.

*Present address: Quantum Brilliance GmbH 5.0G, Industriestrasse 4, 70565 Stuttgart, Germany.

[1] P. Meystre and M. Sargent III, *Elements of Quantum Optics*, 4th ed. (Springer-Verlag, Berlin, Heidelberg, 2007).

- [2] M. A. Nielsen and I. L. Chuang, *Quantum Computation and Quantum Information* (Cambridge University Press, Cambridge, England, 2000).
- [3] J. Stolze and D. Suter, *Quantum Computing: A Short Course from Theory to Experiment*, 2nd ed. (Wiley-VCH, Berlin, 2008).
- [4] J. B. Altepeter, D. F. V. James, and P. G. Kwiat, *Lect. Notes Phys.* **649**, 113 (2004).
- [5] J. B. Altepeter, E. R. Jeffrey, and P. G. Kwiat, *Adv. At. Mol. Opt. Phys.* **52**, 105 (2005).
- [6] I. Chuang, N. Gershenfeld, M. Kubinec, and D. Leung, *Proc. R. Soc. A* **454**, 447 (1998).
- [7] D. G. Cory, A. F. Fahmy, and T. F. Havel, *Proc. Natl. Acad. Sci. U.S.A.* **94**, 1634 (1997).
- [8] G. M. Leskowitz and L. J. Mueller, *Phys. Rev. A* **69**, 052302 (2004).
- [9] J. Wrachtrup and F. Jelezko, *J. Phys. Condens. Matter* **18**, S807 (2006).
- [10] R. R. Ernst, G. Bodenhausen, and A. Wokaum, *Principles of Nuclear Magnetic Resonance in One and Two Dimensions* (Oxford University Press, Oxford, 1987).
- [11] L. M. K. Vandersypen and I. L. Chuang, *Rev. Mod. Phys.* **76**, 1037 (2005).
- [12] L. M. K. Vandersypen, I. L. Chuang, and D. Suter, *Liquid-State NMR Quantum Computing* (John Wiley & Sons, Ltd, New York, 2010).
- [13] M. W. Doherty, N. B. Manson, P. Delaney, F. Jelezko, J. Wrachtrup, and L. C. L. Hollenberg, *Phys. Rep.* **528**, 1 (2013).
- [14] D. Suter and F. Jelezko, *Prog. Nucl. Magn. Reson. Spectrosc.* **98–99**, 50 (2017).
- [15] P. Neumann, N. Mizuochi, F. Rempp, P. Hemmer, H. Watanabe, S. Yamasaki, V. Jacques, T. Gaebel, F. Jelezko, and J. Wrachtrup, *Science* **320**, 1326 (2008).
- [16] T. D. Ladd, F. Jelezko, R. Laflamme, Y. Nakamura, C. Monroe, and J. L. O'Brien, *Nature (London)* **464**, 45 (2010).
- [17] M. Blencowe, *Nature (London)* **468**, 44 (2010).
- [18] J. Cai, F. Jelezko, and M. B. Plenio, *Nat. Commun.* **5**, 4065 (2014).
- [19] G. Kurizki, P. Bertet, Y. Kubo, K. Mølmer, D. Petrosyan, P. Rabl, and J. Schmiedmayer, *Proc. Natl. Acad. Sci. U.S.A.* **112**, 3866 (2015).
- [20] J. F. Barry, J. M. Schloss, E. Bauch, M. J. Turner, C. A. Hart, L. M. Pham, and R. L. Walsworth, *Rev. Mod. Phys.* **92**, 015004 (2020).
- [21] M. Howard, J. Twamley, C. Wittmann, T. Gaebel, F. Jelezko, and J. Wrachtrup, *New J. Phys.* **8**, 33 (2006).
- [22] J. Zhang, A. M. Souza, F. D. Brandao, and D. Suter, *Phys. Rev. Lett.* **112**, 050502 (2014).
- [23] J. J. Longdell and M. J. Sellars, *Phys. Rev. A* **69**, 032307 (2004).
- [24] L. Rippe, B. Julsgaard, A. Walther, Y. Ying, and S. Kroll, *Phys. Rev. A* **77**, 022307 (2008).
- [25] See Supplemental Material at <http://link.aps.org/supplemental/10.1103/PhysRevLett.130.090801> for more details on the qubit systems, additional experimental data for the QST, pulse sequences to implement the unitary transformations required for the QST, and additional information for the QST in 2 qubits, which includes Refs. [26–33].
- [26] K. R. K. Rao and D. Suter, *Phys. Rev. B* **94**, 060101(R) (2016).
- [27] C. S. Shin, M. C. Butler, H.-J. Wang, C. E. Avalos, S. J. Seltzer, R.-B. Liu, A. Pines, and V. S. Bajaj, *Phys. Rev. B* **89**, 205202 (2014).
- [28] X.-F. He, N. B. Manson, and P. T. H. Fisk, *Phys. Rev. B* **47**, 8816 (1993).
- [29] B. Yavkin, G. Mamin, and S. Orlinskii, *J. Magn. Reson.* **15**, 262 (2016).
- [30] J. Zhang, S. S. Hegde, and D. Suter, *Phys. Rev. A* **98**, 042302 (2018).
- [31] A. M. Souza, G. A. Alvarez, and D. Suter, *Phil. Trans. R. Soc. A* **370**, 4748 (2012).
- [32] J. Zhang and D. Suter, *Phys. Rev. Lett.* **115**, 110502 (2015).
- [33] J.-S. Lee, *Phys. Lett. A* **305**, 349 (2002).
- [34] F. Jelezko and J. Wrachtrup, *Phys. Status Solidi (a)* **203**, 3207 (2006).
- [35] L. Childress, M. V. Gurudev Dutt, J. M. Taylor, A. S. Zibrov, F. Jelezko, J. Wrachtrup, P. R. Hemmer, and M. D. Lukin, *Science* **314**, 281 (2006).
- [36] X. Wang, C.-S. Yu, and X. Yi, *Phys. Lett. A* **58**, 373 (2008).
- [37] T. Teraji, T. Taniguchi, S. Koizumi, Y. Koide, and J. Isoya, *Appl. Phys. Express* **6**, 055601 (2013).
- [38] J. Zhang, J. H. Shim, I. Niemeyer, T. Taniguchi, T. Teraji, H. Abe, S. Onoda, T. Yamamoto, T. Ohshima, J. Isoya *et al.*, *Phys. Rev. Lett.* **110**, 240501 (2013).
- [39] K. D. Jahnke, B. Naydenov, T. Teraji, S. Koizumi, T. Umeda, J. Isoya, and F. Jelezko, *Appl. Phys. Lett.* **101**, 012405 (2012).
- [40] N. Khaneja, *Phys. Rev. A* **76**, 032326 (2007).
- [41] J. S. Hodges, J. C. Yang, C. Ramanathan, and D. G. Cory, *Phys. Rev. A* **78**, 010303(R) (2008).
- [42] J. Zhang, S. S. Hegde, and D. Suter, *Phys. Rev. Appl.* **12**, 064047 (2019).
- [43] S. S. Hegde, J. Zhang, and D. Suter, *Phys. Rev. Lett.* **124**, 220501 (2020).
- [44] J. Zhang, S. S. Hegde, and D. Suter, *Phys. Rev. Lett.* **125**, 030501 (2020).
- [45] S. S. Hegde, J. Zhang, and D. Suter, *Phys. Rev. Lett.* **128**, 230502 (2022).
- [46] M. Mitchell, *An Introduction to Genetic Algorithms* (MIT Press, Cambridge, MA, USA, 1998).
- [47] G.-Q. Liu, H. C. Po, J. Du, R.-B. Liu, and X.-Y. Pan, *Nat. Commun.* **4**, 2254 (2013).
- [48] Other experiments, such as the measurement of transition frequencies, do not require full QST.
- [49] N. F. Ramsey, *Phys. Rev.* **78**, 695 (1950).
- [50] H. Sosa-Martinez, N. K. Lysne, C. H. Baldwin, A. Kalev, I. H. Deutsch, and P. S. Jessen, *Phys. Rev. Lett.* **119**, 150401 (2017).
- [51] D. H. Mahler, L. A. Rozema, A. Darabi, C. Ferrie, R. Blume-Kohout, and A. M. Steinberg, *Phys. Rev. Lett.* **111**, 183601 (2013).
- [52] L. Zambrano, L. Pereira, S. Niklitschek, and A. Delgado, *Sci. Rep.* **10**, 12781 (2020).
- [53] T. L. Scholten and R. Blume-Kohout, *New J. Phys.* **20**, 023050 (2018).

- [54] I. Hincks, C. Granade, and D. G. Cory, *New J. Phys.* **20**, 013022 (2018).
- [55] H. Singh, Arvind, and K. Dorai, *Phys. Lett. A* **380**, 3051 (2016).
- [56] J. F. Poyatos, J. I. Cirac, and P. Zoller, *Phys. Rev. Lett.* **78**, 390 (1997).
- [57] I. L. Chuang and M. A. Nielsen, *J. Mod. Opt.* **44**, 2455 (1997).
- [58] Y. Sagi, I. Almog, and N. Davidson, *Phys. Rev. Lett.* **105**, 053201 (2010).
- [59] M. Riebe, K. Kim, P. Schindler, T. Monz, P. O. Schmidt, T. K. Korber, W. Hansel, H. Haffner, C. F. Roos, and R. Blatt, *Phys. Rev. Lett.* **97**, 220407 (2006).
- [60] A. Keselman, Y. Glickman, N. Akerman, S. Kotler, and R. Ozeri, *New J. Phys.* **13**, 073027 (2011).